

Tris(carbene) Stabilization of Monomeric Magnesium Cations: A Neutral, Nontethered Ligand Approach

Akachukwu D. Obi, Jacob E. Walley, Nathan C. Frey, Yuen Onn Wong, Diane A. Dickie, Charles Edwin Webster,* and Robert J. Gilliard, Jr.*



Cite This: *Organometallics* 2020, 39, 4329–4339



Read Online

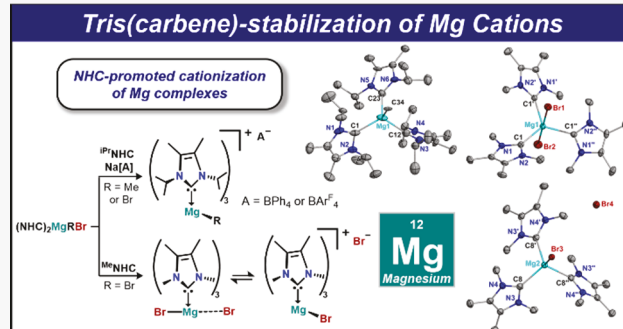
ACCESS |

Metrics & More

Article Recommendations

Supporting Information

ABSTRACT: Herein, we describe the syntheses and structural characterization of bis(carbene)- and tris(carbene)-stabilized organomagnesium cations. The reaction of the N-heterocyclic carbene (NHC) stabilized Grignard reagent $(^{i\text{Pr}}\text{NHC})_2\text{Mg}(\text{Me})(\text{Br})$ (**1**) and $\text{Na}[\text{BAr}^{\text{F}}_4]$ ($^{i\text{Pr}}\text{NHC} = 1,3\text{-diisopropyl-4,5-dimethylimidazol-2-ylidene}$, $\text{Ar}^{\text{F}} = 3,5\text{-bis(trifluoromethyl)phenyl}$) in chlorobenzene yields exclusively the bis(NHC)-stabilized dication $[(^{i\text{Pr}}\text{NHC})_2\text{Mg}(\text{Me})_2](\mu\text{-Me})_2][(\text{BAr}^{\text{F}}_4)_2]$ (**2**). If the reaction is performed in ethereal or nonpolar arene solvents, **2** undergoes Schlenk-type rearrangements to tris(NHC)-stabilized cations $[(^{i\text{Pr}}\text{NHC})_3\text{Mg}(\text{Me})][\text{BAr}^{\text{F}}_4]$ (**3**- $[\text{BAr}^{\text{F}}_4]$) and $[(^{i\text{Pr}}\text{NHC})_3\text{Mg}(\text{Br})][\text{BAr}^{\text{F}}_4]$ (**4**- $[\text{BAr}^{\text{F}}_4]$). These monomeric cations **3**[A] and **4**[A] (A = BAr^{F}_4 , BPh_4) can be independently prepared as single pure products in high yields using common hydrocarbon solvents. The electronic influence of tris(carbene) stabilization is further evidenced by an NHC-mediated ionization of magnesium bromide in the absence of abstraction reagents. The reaction between the sterically unencumbered 1,3,4,5-tetramethylimidazol-2-ylidene ($^{\text{Me}}\text{NHC}$) ligand and $(^{\text{Me}}\text{NHC})_2\text{MgBr}_2$ (**7**) resulted in two geometrically unique cations of the type $[(^{\text{Me}}\text{NHC})_3\text{MgBr}][\text{Br}]$: complex **8a** bearing a weakly coordinating bromide anion resulting in a trigonal bipyramidal magnesium center, and complex **8b** bearing a noncoordinating bromide anion where the magnesium atom resides in a tetrahedral coordination environment. All isolated complexes were characterized by NMR spectroscopy and single-crystal X-ray diffraction, and their bonding was investigated by density functional theory (DFT).



INTRODUCTION

The study of alkaline-earth (Ae) metals in unusual coordination environments is currently experiencing a renaissance, attracting broad interest across the fields of chemical synthesis and catalysis.¹ Indeed, these elements were fairly recently discovered to facilitate stoichiometric and catalytic bond activations when the metal center resides in a low oxidation state or in a bonding situation that renders the metal electrophilic.² Due to the vital importance of electrostatic interactions between alkaline-earth metals and substrates,³ a trend in utilizing charge separation to enhance the electrophilicity of the metal has emerged. The research groups of Harder and Hill have reported an array of β -diketiminate (NacNac)-stabilized cationic alkaline-earth complexes which formed stable, unsupported bonding interactions with a diverse array of arenes, terminal alkynes, silyl ethers, and phosphines.⁴ Notably, these cations have been utilized as frustrated Lewis pair type reagents mediating two-electron dearomatization of benzene,⁵ aromatization of cyclooctatetraene,^{4d} and diverse reactivity at carbon–carbon multiple bonds.^{4f,6}

When alkaline-earth metals bind to the anionic β -diketiminate framework, one electron is immediately consumed in bonding,

leaving one terminal or bridging metal–organic unit. Thus, the formation of electrophilic cations via abstraction of an organic group affords an alkaline-earth center that is free of an exocyclic functional group (excluding weakly coordinating anions, Chart 1). In contrast, the use of L-type neutral ligands for the stabilization of cationic Ae complexes provides a well-defined functional group (e.g., CH_3^-) at the metal.⁷ To this end, N-heterocyclic carbenes (NHCs) are particularly attractive as neutral ancillary ligands, due to their high donor strength, tunable sterics, and electronic flexibility.⁸ However, despite being popular ligands in p-block and transition-metal chemistry, NHC s-block chemistry remains underexplored.⁹ Thus, carbene-stabilized alkaline-earth cations are rare. This is mostly due to the fact that the solution-phase coordination chemistry of such species can be complex, where Schlenk-type ligand

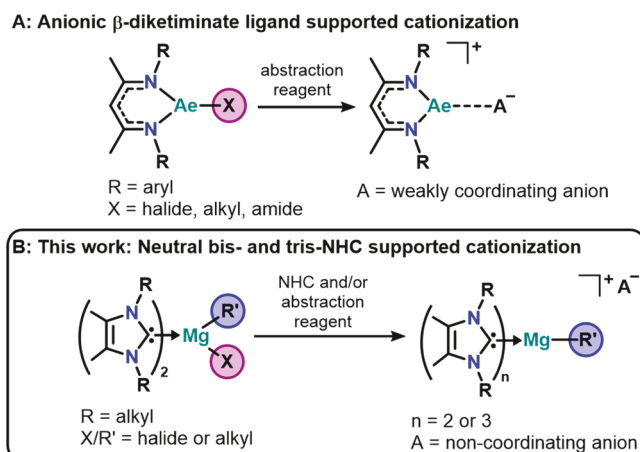
Special Issue: Organometallic Chemistry of the Main-Group Elements

Received: July 7, 2020

Published: August 20, 2020



Chart 1. Bonding Comparison of Neutral and Anionic Ligand-Supported Alkaline-Earth Cations



redistributions and reversible solvent coordination are prominent, especially in their monodentate ligand supported adducts.¹⁰ Nevertheless, recent remarkable advances in carbene-stabilized group 2 organometallics necessitate a reevaluation of the unique potential of NHCs for unusual transformations at these highly electropositive metal centers.^{9d,11}

The utilization of NHCs in group 2 chemistry often requires sterically demanding *N*-aryl substitutions at the carbene to induce kinetic stabilization around the metal center in a manner similar to NacNac-stabilized species. However, we recently initiated studies on the electronic influence of less sterically demanding NHCs on the structure and chemical properties of organoalkaline-earth reagents.¹² Employing a dual NHC coordination strategy with 1,3-diisopropyl-4,5-dimethylimidazol-2-ylidene (^{iPr}NHC), we isolated the first carbene-stabilized terminal Grignard reagent (i.e., (^{iPr}NHC)₂MgMeBr (**1**)) along with a series of unsolvated monomeric magnesium alkyls and halides.^{12a} This system resulted in persistent ligand coordination in contrast to dynamic solvent interaction observed in the mono-NHC-stabilized magnesium complexes.^{7c,12a,13} We now report the syntheses and structural characterization of solvent-free organomagnesium cations stabilized by a nontethered multicarbene system. Notably, complexes **2–5** and **8** represent the first examples of cationic organomagnesium complexes benefiting from bis- and tris(carbene) stabilization.¹⁴ Solvent-dependent ligand rearrangements from bis(NHC)- to tris(NHC)-stabilized cations are also observed. The electronic influence of multiple carbene on magnesium halides is demonstrated in the carbene-mediated cationization of magnesium bromide in the absence of halide abstraction reagents, resulting in the remarkable isolation of geometrically

unique Mg cations (**8a,b**) of the type $[({}^{\text{Me}}\text{NHC})_3\text{MgBr}][\text{Br}]$ (${}^{\text{Me}}\text{NHC} = 1,3,4,5\text{-tetramethylimidazol-2-ylidene}$).

RESULTS AND DISCUSSION

A Bis(N-heterocyclic carbene)-Stabilized Magnesium Dication

The bis-NHC Grignard reagent (^{iPr}NHC)₂MgMeBr (**1**)^{12a} was treated with Na[BAr^F₄] (Ar^F = 3,5-bis(trifluoromethyl)phenyl) in chlorobenzene to afford compound **2** as a colorless solid in 63% yield (Scheme 1). The ¹H NMR spectrum of **2** in C₆D₅Br is consistent with two chemically equivalent ^{iPr}NHC ligands stabilizing a cationic Mg–Me fragment, where the characteristic carbene and methyl protons all resonate upfield of those of **1** (e.g., $\delta(\text{Mg–CH}_3) = 1.02$ ppm for **2** and -0.82 ppm for **1**).

The molecular structure of **2** was unambiguously determined by single-crystal X-ray diffraction, which revealed a dinuclear complex where the Mg atoms are each stabilized by two ^{iPr}NHC ligands and dissymmetrically bridged by their methyl substituents (Figure 1). The resulting dication is balanced by two

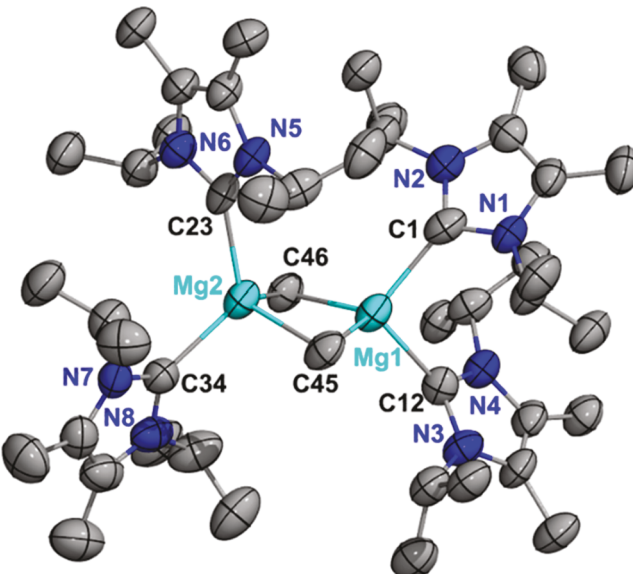
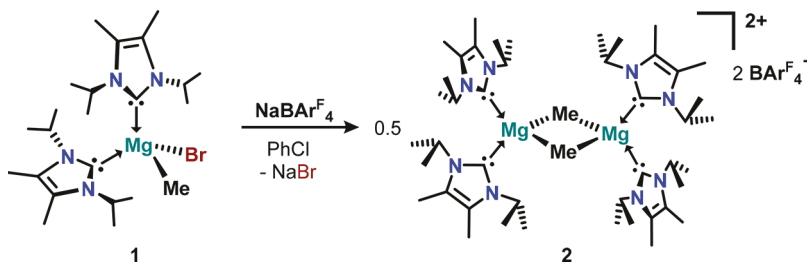


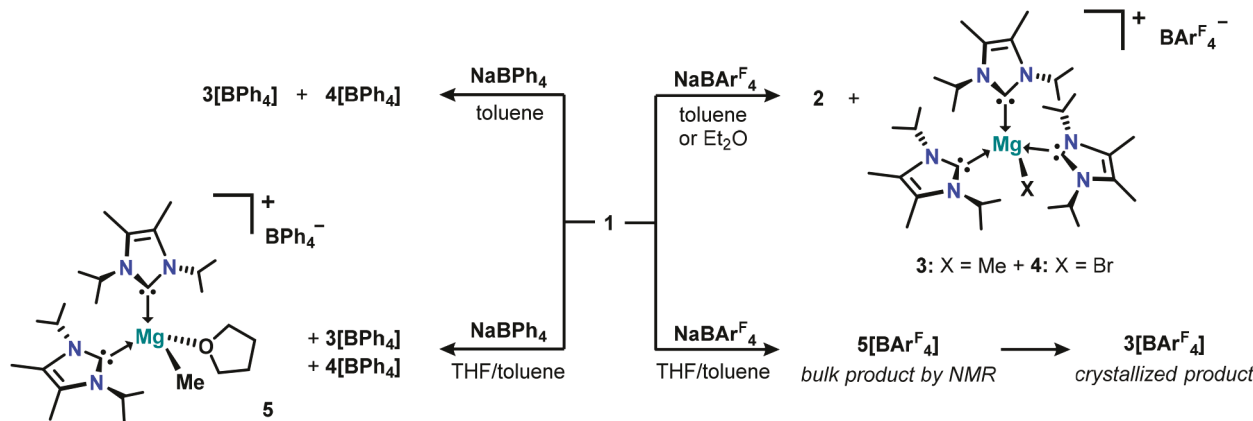
Figure 1. Molecular structure of **2**. Thermal ellipsoids are shown at 50% probability. H atoms, BAr^F₄ anions, and one cocrystallized chlorobenzene solvent molecule are omitted for clarity.

noncoordinating BAr^F₄ anions, indicating that the formation of the [Mg(μ-Me)]₂²⁺ core (Mg–Mg 2.737(4) Å) is preferred over anion or arene solvent interactions. The NHC–Mg bond distances (2.209(10)–2.233(12) Å) are slightly shortened from **1** (2.258(3) and 2.261(3) Å) and are in the range of reported examples.^{12a–d,13} The Mg–(μ-Me) interactions (average

Scheme 1. Synthesis of a Bis(N-heterocyclic carbene)-Stabilized Magnesium Dication



Scheme 2. Ligand Rearrangements of Bis(carbene) to Tris(carbene) Species: Solvent and Borate Anion Stabilization Effects



2.242(11) Å) are shorter than the terminal Mg–Me bond in **1** (2.277(5) Å), likely due to the dicationic nature of **2**. In contrast to similar homometallic organomagnesium complexes which feature planar dimers,¹⁵ the $[\text{Mg}(\mu\text{-Me})_2]^{2+}$ core in **2** exhibits a distorted metallacyclobutane “butterfly” configuration (Mg1–C46–Mg2 74.3(3)°, C45–Mg1–C46 102.7(4)°), where both Mg atoms lie slightly above the C46–Mg2–C45–Mg1 plane (torsion angle of 17.2(4)°) and the methyl groups slightly below. This rare distortion has been observed within an octamethyltrimagnesiate dianion.¹⁶

Ligand Rearrangements of Bis- to Tris(N-heterocyclic carbene)-Stabilized Magnesium Cations. The reaction between **1** and $\text{Na}[\text{BArF}_4]$ in toluene or diethyl ether yielded a mixture of **2** and the tris(NHC)-coordinated species $[(^{\text{Pr}}\text{NHC})_3\text{Mg}(\text{Me})][\text{BArF}_4]$ (**3** [BArF_4]) and $[(^{\text{Pr}}\text{NHC})_3\text{Mg}(\text{Br})][\text{BArF}_4]$ (**4** [BArF_4])) via Schlenk-type ligand rearrangements (Scheme 2). In notable contrast, the reaction of **1** and $\text{Na}[\text{BPh}_4]$ in toluene afforded exclusively the tris(carbene)-coordinated products **3** [BPh_4] and **4** [BPh_4]. These observations suggest that the BArF_4 anions stabilize the formation of **2**, possibly due to intermediary $[\text{Mg}]^+ \cdots \text{F}(\text{BArF}_4)$ contacts prior to dimerization to the dication. Similarly, the utilization of halogenated arene solvents may provide further halide-contact stabilization, as previously observed for cationic alkaline-earth complexes.^{4a} Therefore, we expect that the combined stabilizing effects of the BArF_4 anion and chlorobenzene influenced the isolation of **2** as a pure product (Scheme 1).

We further investigated the influence of THF solvation on the isolation of these cations. The reaction between **1** and $\text{Na}[\text{BPh}_4]$ in THF or a toluene/THF mixture yielded a complex mixture of products, including $[(\text{THF})(^{\text{Pr}}\text{NHC})_2\text{Mg}(\text{Me})][\text{BPh}_4]$ (**5** [BPh_4])) and the tris(NHC) species **3** [BPh_4] and **4** [BPh_4] as observed by NMR. Recrystallization of this mixture in bromobenzene/hexanes yielded colorless crystals identified by X-ray diffraction as the expected monomeric structure, which also included $[(^{\text{Pr}}\text{NHC})_2(\text{THF})\text{Mg}(\text{Br})][\text{BPh}_4]$ in 4% population (Figure 2). Notably, the bulk solid recovered from the reaction between **1** and $\text{Na}[\text{BArF}_4]$ in THF was spectroscopically determined to be the single species **5** [BArF_4]. However, **5** [BArF_4] rearranges and crystallizes from a concentrated THF/toluene mixture as the tris(NHC) species **3** [BArF_4] over 2 days at room temperature.

Gas-phase DFT (ω B97X-D/BS1) suggests a thermodynamic preference for the formation of **3** (−55.1 kcal/mol relative to **1**) over the bis(NHC) complexes **2** (−40.3 kcal/mol) and **5** (−41.4 kcal/mol, Figure S25). In contrast, the inclusion of

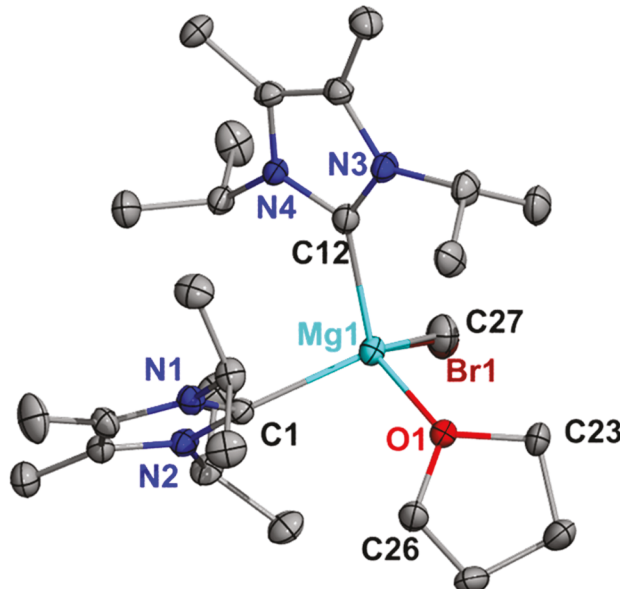
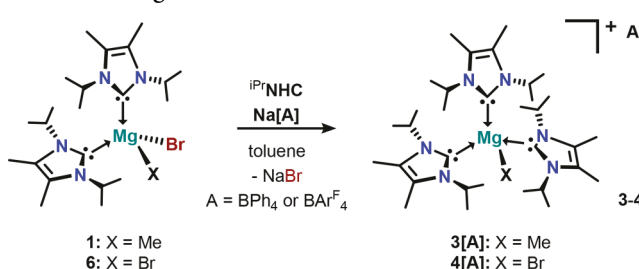


Figure 2. X-ray structure of **5** [BPh_4] including 4% cocrystallized $[(^{\text{Pr}}\text{NHC})_2(\text{THF})\text{Mg}(\text{Br})][\text{BPh}_4]$. Thermal ellipsoids are shown at 50% probability. H atoms and the BPh_4 anion are omitted for clarity. Selected bond distances and angles are shown in Table 1.

solvation models for toluene resulted in a preference for **5** (−80.0 kcal/mol) over **3** (−33.1 kcal/mol), highlighting the observed stabilization of THF-coordinated bis(NHC) cations in the solvent. In addition to the dynamic THF coordination observed, the rearrangements in **5** are perhaps unsurprising, as coordinating solvents play a significant role in Schlenk-type ligand redistributions.¹⁷ Therefore, we targeted the solvent-free tris(NHC)-stabilized cations as single products using common hydrocarbon solvents.

Direct Syntheses and Structural Analyses of Tris(N-heterocyclic carbene)-Stabilized Magnesium Cations. Colorless crystalline solids of complexes **3** and **4** were isolated in 49–80% yields by combining $(^{\text{Pr}}\text{NHC})_2\text{Mg}(\text{X})(\text{Br})$ (**1**, X = Me; **6**, X = Br),^{12a} $^{\text{Pr}}\text{NHC}$, and $\text{Na}[\text{BArF}_4]$ or $\text{Na}[\text{BPh}_4]$ in toluene (Scheme 3). Evidence of donor-rich metal centers can be found in higher-field resonances of the carbene methine protons (δ 4.72 for **3** [BArF_4] and δ 4.73 for **3** [BPh_4] in C_6D_6) with respect to **1** (δ 5.62). The nearly identical methine resonances in **3** are similarly observed for **4** (δ 4.90 for both **4** [BArF_4] and **4** [BPh_4] in CD_2Cl_2). This suggests that the

Scheme 3. Syntheses of Tris(N-heterocyclic carbene)-Stabilized Magnesium Cations



nature of the noncoordinating anion does not significantly influence the electronics in these tris(carbene)-stabilized magnesium cations. The methyl protons in $3[BAr^F_4]$ (δ -0.90) and $3[BPh_4]$ (δ -0.86) are significantly upfield of 1 (δ -0.45), suggesting increased nucleophilicity from the neutral Grignard.

Suitable single crystals of $3[BAr^F_4]$, $3[BPh_4]$, $4[BAr^F_4]$, and $4[BPh_4]$ were obtained and analyzed by X-ray diffraction, revealing the expected mononuclear complexes (Figure 3 and Figures S1 and S2). Each structure maintains a distorted tetrahedral geometry around the magnesium cation, which is stabilized by three iPr NHC ligands and one noncoordinating borate anion. The ^{NHC}C –Mg distances in 3 and 4 (see Table 1) are also comparable to those in 2 and the neutral bis-NHC complexes. The similarity in ^{NHC}C –Mg distances for $3[BAr^F_4]$ [(2.262(5), 2.276(6), 2.281(6) Å) is reflected in the geometry around the magnesium atom, where the bond angles (103.6–112.2°) only slightly deviate from the ideal 109.5° of a perfect tetrahedron. A detailed comparison of structural parameters for 2–5 is summarized in Table 1.

Compound 3 may also be prepared using THF, thus indicating that tris(NHC) stabilization affords the electronic benefit of persistent carbene coordination, which is competitive against donor solvents. In contrast, compound 4 is substantially more sensitive than 3 to adventitious moisture in THF, despite considerable effort to rigorously dry the reaction solvents. Therefore, crystallization of hydrolysis products of the type $[(^{iPr}NHC)H][BR_4]$ ¹⁸ ($R = Ph, Ar^F$) from THF solutions of 4 was consistently observed. Additionally, $3[BPh_4]$ displays significantly improved solubility in arene solvents in comparison

to 2 , thus rendering it a more practical alternative for synthetic applications where donor solvents should be avoided. Notably, compounds 2 – 4 are stable as solids in an inert atmosphere for at least 3 months at room temperature and up to 2 weeks in anhydrous arene solvents at -37 °C.

N-heterocyclic Carbene Mediated Heterolysis of Magnesium Bromide. To further probe the electronic influence of multiple NHCs on magnesium complexes, we investigated the ionization of magnesium bromide ($MgBr_2$) in the absence of halide abstraction reagents. In order to maximize donor interactions with the metal center, the sterically unencumbered 1,3,4,5-tetramethylimidazol-2-ylidene (^{Me}NHC) ligand¹⁹ was chosen for this investigation. Similar to the case for 6 ,^{12a} the neutral bis-NHC species $(^{Me}NHC)_2MgBr_2$ (7) was obtained as a colorless solid in 84% yield from the addition of 2 equiv of ^{Me}NHC to $MgBr_2$ in toluene (Scheme 4). The X-ray structure of 7 (Figure 4 and Table 1) reveals metrical parameters comparable to those of 6 .

Starting from a suspension of 7 in chlorobenzene, the addition of 1 or 2 equiv of ^{Me}NHC immediately yielded a colorless solution (Scheme 4). The 1H NMR of the isolated product in C_6D_5Br revealed a single NHC coordination environment (two singlets at δ 3.55 and 1.60) with the α -CH₃ resonance (δ 3.55) being significantly broadened. This suggests a possible dynamic equilibrium in solution, although the existence of more than one unique species in solution could not be resolved using variable-temperature (VT) NMR experiments (C_6D_5Br , 373–248 K). Access to lower temperatures was limited by the freezing point of C_6D_5Br (-30.7 °C) and the overall poor solubility of this compound in common organic solvents. However, single-crystal X-ray diffraction studies revealed that two distinct molecules, $8a$ and $8b$, cocrystallized in the solid state in a 1:1 ratio (Figure 5).

Complex $8a$ is an unusual trigonal bipyramidal magnesium complex stabilized by three ^{Me}NHC ligands in the equatorial plane and two Br ligands in the axial positions. The Mg–Br distances in $8a$ (2.694(3) and 2.883(3) Å) are significantly elongated by 0.18–0.40 Å from the neutral bis(NHC) complex 7 (2.487(3) and 2.510(3) Å), as well as the expected additive covalent radii between Mg and Br (2.53 Å).²⁰ Thus, $8a$ may be considered as either a neutral L_3MgBr_2 complex or a cationic magnesium complex stabilized by a weakly coordinating bromide anion. In contrast, $8b$ can only be described as an

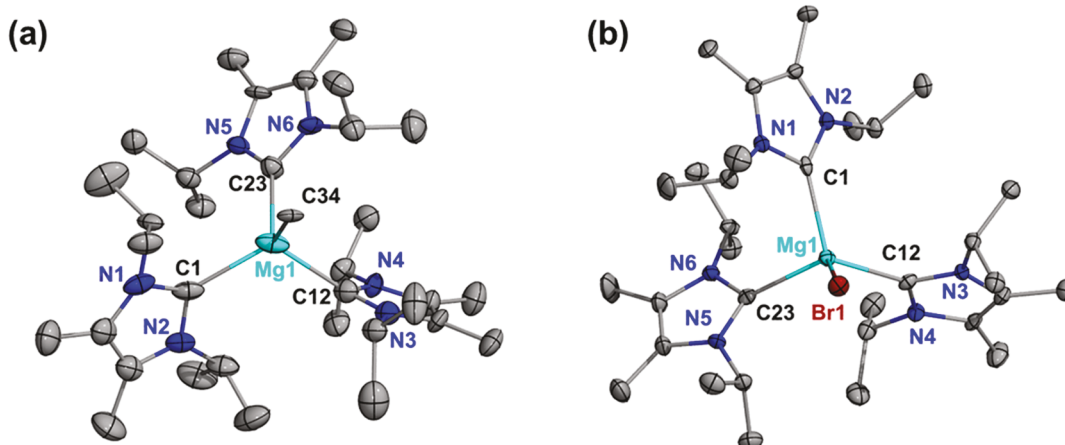
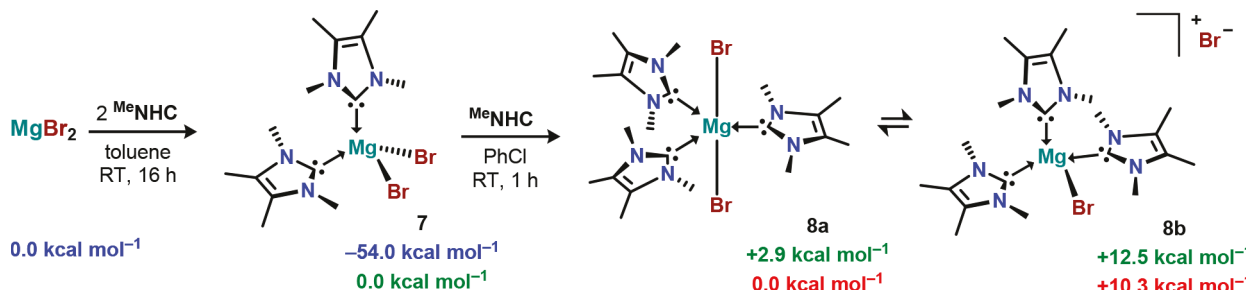


Figure 3. X-ray structures of BPh_4 salts for 3 (a) and 4 (b). Thermal ellipsoids are shown at 50% probability. H atoms and anions are hidden for clarity. Only the major occupied positions are shown for the disordered C12 and C23 imidazole frameworks and *N*-isopropyl substituents in (a). $3[BAr^F_4]$ (Figure S1) and $4[BAr^F_4]$ (Figure S2) are shown in the Supporting Information.

Table 1. Selected Bond Distances^a and Angles^b for Compounds 2–5, 7, and 8

	2	3[BAr ^F ₄]	3[BPh ₄]	4[BAr ^F ₄]	4[BPh ₄]	5[BPh ₄]	7	8a	8b
^{NHC} C–Mg	2.233(12)	2.262(5)	2.277(2)	2.2360(18)	2.209(3)	2.260(2)	2.234(13)	2.214(5)	2.215(5)
	2.209(10)	2.276(6)	2.163(7)	2.2554(18)	2.210(3)	2.246(3)	2.217(13)		
	2.228(10)	2.281(6)	2.271(2)	2.2434(18)	2.251(3)				
	2.212(11)								
^{Me} C–Mg	2.223(11)	2.154(5)	2.2557(19)			2.178(14)			
	2.246(10)								
	2.215(10)								
	2.285(11)								
Mg1–Br1				2.4934(6)	2.5195(9)		2.510(3)	2.883(3)	2.513(3) ^c
Mg1–Br2							2.487(3)	2.694(3)	
C1–N1	1.363(13)	1.364(7)	1.369(3)	1.360(2)	1.394(3)	1.365(3)	1.333(13)	1.361(7)	1.348(7) ^d
C1–N2	1.356(13)	1.376(6)	1.391(3)	1.360(2)	1.364(3)	1.360(3)	1.339(13)	1.361(7)	1.359(7) ^e
C1–Mg1–C12	100.1(4)	108.85(19)	114.5(3)	113.16(6)	115.3(11)	99.32(9)	108.9(4) ^h	119.77(3) ^h	109.70(15) ^f
C1–Mg1–C23		111.4(2)	108.76(7)	107.38(6)	101.59(10)	98.60(8) ⁱ			
C1–Mg1–X ^j	115.7(4)	109.8(2)	112.87(7)	107.99(5)	107.33(8)	107.1(4)	106.3(3)	87.25(16)	109.24(15) ^g
								108.0(3)	92.75(16)
X ¹ –Mg–X ²	102.7(4)						119.41(11)	180.00(6)	
	101.7(4)								
N1–C1–N2	104.5(9)	103.2(4)	102.54(17)	103.94(14)	104.1(2)	103.51(19)	104.9(10)	102.6(4)	104.0(4)

^aIn angstroms. ^bIn degrees. ^cMg2–Br3. ^dC8–N3. ^eC8–N4. ^fC8–Mg2–C8'. ^gC8–Mg2–Br3. ^hC8 (7) and C1' (8a) were used instead of C12. ⁱO1 was used instead of C23 for 5[BPh₄]. ^jX represents Me or Br where applicable.

Scheme 4. NHC-Mediated Heterolysis of MgBr₂: Syntheses and Calculated Reaction Energetics^a

^aSMD- ω B97X-D// ω B97X-D/BS1 reaction energetics (ΔG) using implicit solvation models for toluene (blue values), chlorobenzene (green values), and bromobenzene (red values) solvents.

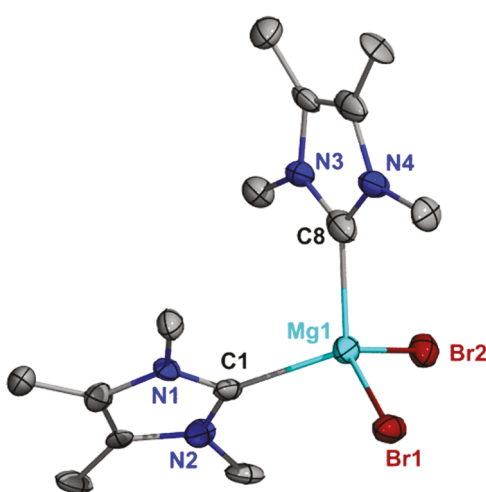


Figure 4. X-ray structure of 7. Thermal ellipsoids are shown at 50% probability. H atoms are omitted for clarity.

ionic [L₃MgBr][Br] complex. The crystal structure of 8b reveals a tetracoordinate magnesium cation stabilized by three carbenes and a bromide ligand, with the second bromide acting as a

noncoordinating anion. The closest contact between Mg2 and the noncoordinating bromide, Br4 (6.374(2) Å) is nearly double the expected van der Waals separation between Mg and Br (3.56 Å).²¹ The Mg2–Br3 bond length in 8b (2.513(3) Å) is significantly shorter than those of 8a but is comparable to those of 4 and 7 (see Table 1). In both 8a and 8b, a crystallographic 3-fold rotation axis passes through the Mg–Br bond, and only one carbene is found in the asymmetric unit of each species. Thus, the ^{NHC}C–Mg bond distances for 8a (2.214(5) Å) and 8b (2.215(5) Å) are similarly identical. This results in a D_{3h} symmetry for 8a where Br1–Mg–Br2 is exactly 180° and the ^{NHC}C–Mg–^{NHC}C angles are each 120°, as well as a C_{3v} symmetry for the cationic fragment in 8b, which maintains a nearly perfect tetrahedral geometry (109.24–109.70(15)°) around the magnesium center.

Complexes 1 and 6 were found to be unreactive with ^{iPr}NHC under conditions similar to those for the reaction of 7 with ^{Me}NHC, likely due to steric hindrance from the isopropyl groups. This indicates that the formation of 3 and 4 proceeded via initial halide abstraction followed by carbene coordination. Theoretical calculations (SMD(chlorobenzene)- ω B97X-D// ω B97X-D/BS1) suggest a small energy penalty of +2.9 kcal mol⁻¹ for the formation of 8a by complexation of an additional

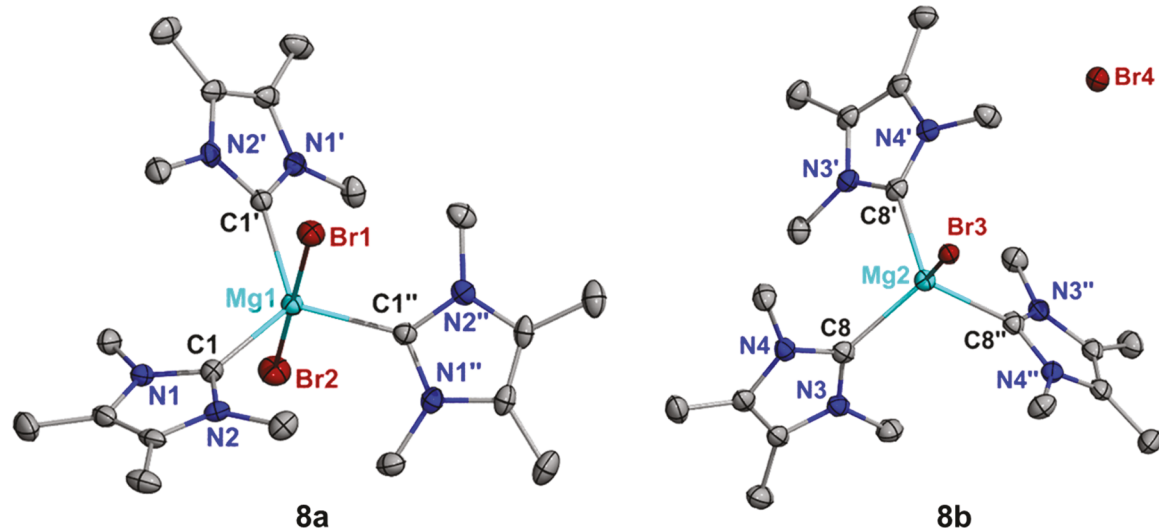


Figure 5. X-ray structures of **8a** and **8b**. Thermal ellipsoids are shown at 50% probability. H atoms are omitted for clarity.

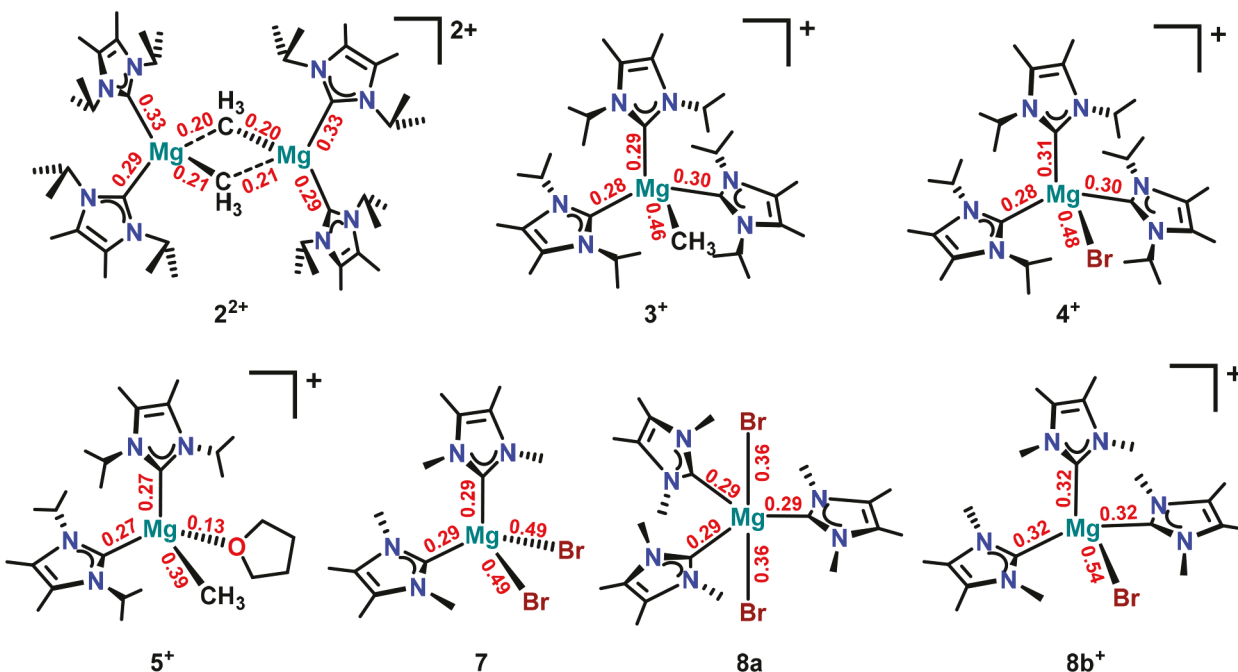


Figure 6. Comparison of NAO-Wiberg bond index (WBI) values for each reported compound.

NHC to **7**. Further displacement of a weakly coordinating bromide ligand to form **8b** is calculated to be endergonic by 9.6 kcal mol⁻¹, thus indicating a thermodynamic preference for **8a** in the suggested equilibrium. Nevertheless, the existence of **8a** and **8b** in the solid state indicates that multiple NHCs can easily ionize neutral magnesium complexes containing halides. The unique geometry of **8a**, owing to the use of sterically unencumbered carbenes, indicates that the magnesium center may be able to accommodate additional carbenes to access further ionized or polarized species. Ionization of the remaining covalent Mg–Br interaction using excess carbenes, extended reaction times, or halide abstraction reagents has resulted in species spectroscopically dissimilar from **7** and **8**, but their poor solubility hindered successful crystallization attempts. Likewise, we explored an alternate route to **8** by the direct addition of 3 equiv of ^{Me}NHC to a suspension of MgBr₂ in toluene. The resulting complex was spectroscopically comparable to **8** (δ 3.57

(broad) and 1.60), thereby indicating that the direct heterolysis of polymeric MgBr₂ could be achieved without initial isolation of the neutral bis(NHC)-stabilized species.

Theoretical Analysis. In order to gain more insight into the structure and bonding of the bis- and tris(NHC) magnesium systems, DFT geometry optimizations were performed at the ω B97X-D/BS1 level of theory. Overall, the Wiberg bond index (WBI) values computed for the ^{NHC}C–Mg bonds in the cationic complexes (Figure 6) are comparable to those of the neutral bis-NHC complexes,^{12a} with only slight increase in values, which are most pronounced for **2²⁺** (0.29 and 0.33) and **8b⁺** (0.32).

Relative to their neutral precursors, higher Mg–X WBI values are generally observed for the cationic complexes. The Mg–Me bond in **3⁺** (WBI 0.46) displays a greater degree of covalency in comparison to those in **1** (0.37) and **5⁺** (0.39). The lower WBIs for the Mg–(μ-Me) bonds in **2²⁺** (0.21, 0.20) relative to the terminal Mg–Me bonds in **1**, **3**, and **5** suggest a significantly

greater degree of charge separation between the Mg cations and bridging methyl anions. This observation is further supported by an inspection of the natural charges (Table S2) and Pipek-Mezey localized molecular orbitals for the Mg-(μ -Me) interactions in **2²⁺** (Figure S31). Expectedly, the WBI value for Mg-Br in (^{Me}NHC)₂MgBr₂ (**7**) is the same as that previously reported for (^{iPr}NHC)₂MgBr₂.^{12a} However, the value for the Mg-Br bond in the ^{iPr}NHC-stabilized cation **4⁺** (0.48) is lower than that of the ^{Me}NHC-stabilized cation **8b⁺** (0.54), despite only slight differences in their ^{NHC}C-Mg WBI values (**4⁺**: 0.28, 0.30, 0.31; **8b⁺**: 0.32). The larger difference in WBI values for the Mg-Br bonds in **8a** (0.36) and **8b⁺** (0.54), which are on either side of **7** (0.49), corroborates the weakly coordinating nature of the bromide anions in **8a**.

CONCLUSION

We have isolated the first examples of organomagnesium cations benefiting from untethered bis- and tris(carbene) stabilization. The bis(NHC)-stabilized complexes exhibited solvent-dependent Schlenk-type ligand rearrangements to hitherto unknown organomagnesium complexes benefiting from unsupported tris(carbene) stabilization. The facile and high yielding syntheses of **3** and **4** demonstrate that tris(carbene)-supported ionization using easily accessible halide abstraction reagents can be extended to other magnesium halide systems. We further explored the electronic influence of tris(carbene) stabilization in the NHC-mediated heterolysis of polymeric magnesium bromide. These types of solvent-free, base-saturated species are expected to have beneficial applications in molecular alkaline-earth reduction chemistry²² and small molecule activation.^{1a,7a,23} Thus, investigations into the reactivity of these cations with hydride sources, small molecule substrates and reducing agents are currently underway and will be reported in due course.

EXPERIMENTAL SECTION

General Considerations. All manipulations were carried out under an atmosphere of purified argon using standard Schlenk techniques or in a MBRAUN LABmaster glovebox equipped with a-37 °C freezer and operating at <0.1 ppm of H₂O and O₂. Glassware were oven-dried at 190 °C overnight. Halogenated solvents (dichloromethane, bromobenzene, and chlorobenzene) were purified by distillation over calcium hydride for at least 48 h and degassed with 3X freeze-pump-thaw cycles. Toluene, hexanes, and THF were distilled over sodium. Deuterated solvents were purchased from Acros Organics and Cambridge Isotope Laboratories and dried the same way as their protic analogues. The NMR spectra were recorded on the following instruments: a Varian Inova 500 MHz (¹H, 500.13 MHz), a Varian NMRS 600 MHz (¹H, 600 MHz; ¹³C, 150.90 MHz; ¹¹B NMR, 192.55 MHz), and a Bruker Avance III 800 MHz (¹H, 800.13 MHz; ¹³C, 201.19 MHz). Proton and carbon chemical shifts are reported in ppm and are referenced to SiMe₄ using the residual proton and carbon signals of the deuterated solvent (¹H, C₆D₆, δ 7.16; ¹³C, C₆D₆, δ 128.06; ¹H, CD₂Cl₂, δ 5.32; ¹³C, CD₂Cl₂, δ 53.84, ¹H, C₆D₅Br, δ 6.95 (*m*-H); ¹³C, C₆D₅Br, δ 122.21). Boron chemical shifts were referenced using an external standard (¹¹B, BF₃·Et₂O, δ 0.0). Data are ordered as follows: chemical shift, multiplicity (s = singlet, d = doublet, t = triplet, q = quartet, sept = septet, m = multiplet, br = broad), coupling constants (*J*/Hz), and integration. X-ray intensity data were measured on a Bruker Kappa APEXII Duo system. An Incoatec Microfocus 1μ S (Cu $K\alpha$, λ = 1.54178 Å) and a multilayer mirror monochromator were used for **2**, **3[BAr^F]₂**, **4[BAr^F]₂**, **5[BPh₄]₂**, and **8**, and a fine-focus sealed tube (Mo $K\alpha$, λ = 0.71073 Å) and a graphite monochromator were used for **3[BPh₄]₂**, **4[BPh₄]₂**, and **7**. Each structure was solved and refined using the Bruker SHELXTL Software Package²⁴ within APEX3²⁵ and

OLEX2.²⁶ Crystallographic data are summarized in Table S1. Anhydrous MgBr₂ (98%, Strem Chemicals) and Na[BPh₄] (>99.5%, Sigma-Aldrich) were used as received. Na[BAr^F]₂,²⁷ ^{iPr}NHC,¹⁹ and ^{Me}NHC^{19,28} were prepared according to literature and recrystallized before use. (^{iPr}NHC)₂MgMeBr (**1**) and (^{iPr}NHC)₂MgBr₂ (**6**) were prepared as previously reported.^{12a} Elemental analyses yielded overall unsatisfactory results due to the extreme air and moisture sensitivity of these compounds. Similar challenges with determining the purity of group 2 complexes using combustion microanalysis have been well documented.^{13,29} Therefore, NMR spectroscopy was used to determine bulk purity, and the spectra of all compounds are provided in the Supporting Information.

Synthesis of [(^{iPr}NHC)₂Mg]₂(μ -Me)₂[(BAr^F)₂]₂, (2**).** In a 20 mL scintillation vial, a chlorobenzene solution (5 mL) of Na[BAr^F]₂ (93 mg, 0.105 mmol) was added dropwise to a stirred solution of **1** (50 mg, 0.104 mmol) in the same solvent. After 3 h, trace solids presumed to be NaBr were removed via filtration. The recovered light bronze solution was concentrated under reduced pressure before addition of hexanes (3 mL) to precipitate the product as a white solid, which was further washed with hexanes (1 \times 5 mL) and dried under vacuum (83 mg, 63%). X-ray-quality single crystals were grown from a concentrated C₆H₅Cl/hexanes solution of **2** in a -37 °C freezer. Notably, **2** may also be prepared using the ether solvate Na[BAr^F]₂·3.5Et₂O. ¹H NMR (500 MHz, C₆D₅Br, 398 K): δ 8.07 (s, 8H, Ar(*o*-H)), 7.61 (s, 4H, Ar(*p*-H)), 4.30 (br s, 4H, CH-*iPr*), 1.86 (s, 12H, C(CH₃)), 1.21 (d, *J* = 7.0 Hz, 24H), -1.02 (s, 3H, Mg(CH₃)). ¹¹B NMR (192.55 MHz, C₆D₅Br, 398 K): δ -6.02. Due to poor solubility, a sufficiently resolved ¹³C NMR spectrum could not be obtained.

Synthesis of [(^{iPr}NHC)₃MgMe][BAr^F]₄ (3[BAr^F]₂**).** In a 20 mL scintillation vial, free ^{iPr}NHC (19 mg, 0.104 mmol) and **1** (50 mg, 0.104 mmol) were dissolved in toluene (15 mL) and stirred. Then, Na[BAr^F]₂ (93 mg, 0.105 mmol) was added slowly to the cloudy mixture and stirred for 6 h at room temperature. A clear solution was recovered via filtration, and the remaining solids were extracted with additional toluene (5 mL), leaving behind trace off-white solids presumed to be NaBr. The filtrate was concentrated under vacuum and stored at room temperature, yielding large colorless platelike crystals suitable for single-crystal X-ray diffraction. After drying under vacuum, **3[BAr^F]₂** was recovered as a crystalline white solid (120 mg, 80%). Notably, **3[BAr^F]₂** may also be prepared using THF without the formation of solvated products. ¹H NMR (600 MHz, C₆D₆, 298 K): δ 8.33 (s, 8H, Ar(*o*-H)), 7.68 (s, 4H, Ar(*p*-H)), 4.72 (br s, 6H, CH-*iPr*), 1.63 (s, 18H, C(CH₃)), 1.01 (br s, 36H, CH₃-*iPr*), -0.90 (s, 3H, Mg(CH₃)). Due to poor solubility, a sufficiently resolved ¹³C{¹H} NMR could not be obtained in C₆D₆. Although they were successfully characterized in CD₂Cl₂, complexes **3** and **4** slowly convert into unidentified products after 2 h in that solvent. ¹H NMR (600 MHz, CD₂Cl₂, 298 K): δ 7.71 (s, 8H, Ar(*o*-H)), 7.56 (s, 4H, Ar(*p*-H)), 4.84 (sept, *J* = 7.0 Hz, 6H, CH-*iPr*), 2.20 (s, 18H, C(CH₃)), 1.32 (d, *J* = 7.7 Hz, 36H, CH₃-*iPr*), -1.35 (s, 3H, Mg(CH₃)). ¹³C NMR (150.90 MHz, CD₂Cl₂, 298 K): 186.2, 182.6, 135.2, 129.2, 126.3, 125.9, 124.1, 117.9, 22.6, 10.7, -8.9. ¹¹B NMR (192.55 MHz, CD₂Cl₂, 298 K): δ -6.67.

Synthesis of [(^{iPr}NHC)₃MgMe][BPh₄]₂ (3[BPh₄]₂**).** In a 100 mL round-bottomed flask, ^{iPr}NHC (39 mg, 0.219 mmol) and **1** (102 mg, 0.213 mmol) were dissolved in toluene (50 mL) and stirred at room temperature before Na[BPh₄] (80 mg, 0.233 mmol) was added to the cloudy mixture. After 16 h, a colorless solution was recovered via filtration and reduced to incipient recrystallization, yielding large blocklike colorless crystals suitable for X-ray diffraction at room temperature. Solids recovered from filtration were further extracted with toluene (15 mL). After removal of volatiles, **3[BPh₄]₂** was recovered as a crystalline white solid (135 mg, 71% yield). ¹H NMR (600 MHz, C₆D₆, 298 K): δ 8.12 (m, 8H, Ar(*m*-H)), 7.36 (t, *J* = 7.3 Hz, 8H, Ar(*o*-H)), 7.21 (t, *J* = 7.3 Hz, 4H, Ar(*p*-H)), 4.73 (sept, *J* = 7.0 Hz, 6H, CH-*iPr*), 1.66 (s, 18H, C(CH₃)), 1.04 (d, *J* = 7.1 Hz, 36H, CH₃-*iPr*), -0.86 (s, 3H, Mg(CH₃)). ¹³C{¹H} NMR (150.9 MHz, C₆D₆, 298 K): 182.2, 137.5, 126.1, 122.1, 53.2, 22.4, 10.3. ¹H NMR (600 MHz, CD₂Cl₂, 298 K): δ 7.31 (m, 8H, Ar(*m*-H)), 7.02 (t, *J* = 7.5 Hz, 8H, Ar(*o*-H)), 6.87 (t, *J* = 7.2 Hz, 4H, Ar(*p*-H)), 4.84 (sept, *J* = 7.0 Hz, 6H, CH-*iPr*), 2.21 (s, 18H, C(CH₃)), 1.34 (d, *J* = 8.1 Hz, 36H, CH₃-*iPr*),

–1.34 (s, 3H, $\text{Mg}(\text{CH}_3)$). $^{13}\text{C}\{\text{H}\}$ NMR (150.9 MHz, CD_2Cl_2 , 298 K): δ 182.4, 164.7, 136.3, 126.3, 126.0, 122.1, 22.6, 10.8, –8.96. ^{11}B NMR (192.55 MHz, CD_2Cl_2 , 298 K): δ –6.44.

Synthesis of $[(\text{iPrNHC})_3\text{MgBr}][\text{BAr}^{\text{F}}_4]$ (4[BAr^F₄]). The same procedure was followed as for the preparation of 3[BAr^F₄], using $(\text{iPrNHC})_2\text{MgBr}_2$ (57 mg, 0.104 mmol) and the corresponding molar equivalents of iPrNHC (19 mg, 0.104 mmol) and $\text{Na}[\text{BAr}^{\text{F}}_4]$ (93 mg, 0.105 mmol) in toluene. After 6 h, a light bronze solution was recovered via filtration and the expected product further extracted from the precipitated solids using chlorobenzene (5 mL). The solutions recovered were concentrated under vacuum and, upon light agitation, precipitated colorless blocklike crystals, which were further dried under vacuum to obtain 4[BAr^F₄] a colorless solid (76 mg, 49% yield). ^1H NMR (600 MHz, CD_2Cl_2 , 298 K): δ 7.71 (s, 8H, Ar(*o*-H)), 7.56 (s, 4H, Ar(*p*-H)), 4.90 (sept, J = 7.0 Hz, 6H, CH-*iPr*), 2.22 (s, 18H, C(CH₃)), 1.36 (d, J = 7.1 Hz, 36H, CH₃-*iPr*). ^{13}C NMR (150.9 MHz, CD_2Cl_2 , 298 K): δ 177.7, 162.7, 162.3, 162.0, 161.7, 135.2, 129.4, 129.2, 127.7, 127.1, 125.9, 124.1, 117.9, 54.1, 22.6, 10.7. ^{11}B NMR (192.55 MHz, CD_2Cl_2 , 298 K): δ –6.67.

Synthesis of $[(\text{iPrNHC})_3\text{MgBr}][\text{BPh}_4]$ (4[BPh₄]). The same procedure was followed as for the preparation of 3[BAr^F₄], using $\text{Na}[\text{BPh}_4]$ (36 mg, 0.104 mmol) and the corresponding molar equivalents of $(\text{iPrNHC})_2\text{MgBr}_2$ and iPrNHC in toluene. After 3 days, colorless precipitates were collected over a fritted Buchner funnel and dried under vacuum. Due to the poor solubility of the product, NaBr was not removed prior to yield (111 mg, quantitative) and NMR analyses, the latter revealing a single pure product (Figure S14). An aliquot of the product was concentrated in $\text{C}_6\text{H}_5\text{Br}$ and layered with hexanes, yielding X-ray-quality single crystals of 4[BPh₄] at –37 °C. Note: despite rigorous efforts at drying the reaction solvents, the hydrolysis product $[(\text{iPrNHC})\text{H}][\text{BPh}_4]$ ¹⁸ was regularly obtained alongside 4[BPh₄] during crystallization. ^1H NMR (600 MHz, CD_2Cl_2 , 298 K): δ 7.31 (m, 8H, Ar(*m*-H)), 7.02 (t, J = 7.4 Hz, 8H, Ar(*o*-H)), 6.87 (t, J = 7.3 Hz, 4H, Ar(*p*-H)), 4.90 (sept, J = 7.0 Hz, 6H, CH-*iPr*), 2.23 (s, 18H, C(CH₃)), 1.37 (d, J = 7.1 Hz, 36H, CH₃-*iPr*). ^{13}C NMR (150.9 MHz, CD_2Cl_2 , 298 K): δ 186.2, 177.7, 165.0, 136.3, 127.11, 125.99, 125.98, 122.1, 54.1, 22.6, 10.8. ^{11}B NMR (192.55 MHz, CD_2Cl_2 , 298 K): δ –6.60.

Synthesis of $[(\text{iPrNHC})_2(\text{THF})\text{Mg}(\text{Me})][\text{BAr}^{\text{F}}_4]$ (5[BAr^F₄]). A THF (5 mL) solution of $\text{Na}[\text{BAr}^{\text{F}}_4]\cdot 3.5\text{Et}_2\text{O}$ (60 mg, 0.0524 mmol) was added dropwise to a stirred colorless THF (5 mL) solution of 1 (25 mg, 0.0521 mmol) in a 20 mL scintillation vial. After 12 h, a colorless solution was recovered over a 0.45 μm pore syringe filter, and the volatiles were removed under vacuum with trituration/wash using hexanes (4 \times 5 mL). After initial spectroscopic analysis, the off-white solid recovered was concentrated in toluene/THF and crystallized as the tris(carbene) adduct 3[BAr^F₄]. Notably, the THF coordination in the bulk sample 5[BAr^F₄] was found to be persistent against evacuation over several hours. ^1H NMR (600 MHz, $\text{C}_6\text{D}_5\text{Br}$, 298 K): δ 8.33 (s, 8H, Ar(*o*-H)), 7.68 (s, 4H, Ar(*p*-H)), 4.31 (br. s, 4H, CH-*iPr*), 3.46 (s, O(CH₂)-THF), 1.57 (s, 12H, C(CH₃)), 1.36 (s, CH₂(CH₂)-THF), 0.98 (m, 24H, CH₃-*iPr*), –1.04 (s, 3H, $\text{Mg}(\text{CH}_3)$). Due to poor solubility, a sufficiently resolved ^{13}C NMR spectrum could not be obtained.

Synthesis of $[(\text{iPrNHC})_2(\text{THF})\text{MgMe}][\text{BPh}_4]$ (5[BPh₄]). The same procedure was followed as for the preparation of 5[BAr^F₄] using $\text{Na}[\text{BPh}_4]$ (35 mg, 0.104 mmol) instead of $\text{Na}[\text{BAr}^{\text{F}}_4]$. Colorless single crystals suitable for X-ray diffraction were obtained from a $\text{C}_6\text{H}_5\text{Br}$ /hexanes solution. ^1H NMR revealed a complex mixture of 5[BPh₄] and the ligand rearrangement products 3[BPh₄] and 4[BPh₄], and the corresponding resonances were all identified (Figure S24). Notably, this reaction yielded similar results when it was performed with THF/toluene mixtures instead of pure THF. ^1H NMR (600 MHz, CD_2Cl_2 , 298 K): δ 7.30 (m, 8H, Ar(*m*-H)), 7.02 (t, J = 7.4 Hz, 8H, Ar(*o*-H)), 6.87 (t, J = 7.2 Hz, 4H, Ar(*p*-H)), 4.64 (sept, J = 7.1 Hz, 4H, CH-*iPr*), 3.87 (m, 4H, O(CH₂)-THF), 2.19 (s, 12H, C(CH₃)), 1.96 (m, CH₂(CH₂)-THF), 1.40 (d, J = 7.1 Hz, 24H, CH₃-*iPr*), –1.42 (s, 3H, $\text{Mg}(\text{CH}_3)$). Due to unsuccessful attempts to isolate pure samples of 5[BPh₄] from the ligand rearrangement minor products, $^{13}\text{C}\{\text{H}\}$ NMR and yield analyses were not performed.

Synthesis of $(^{\text{Me}}\text{NHC})_2\text{MgBr}_2$ (7). Free $^{\text{Me}}\text{NHC}$ (70 mg, 0.564 mmol) was added to a stirred toluene (15 mL) suspension of MgBr_2 (52 mg, 0.282 mmol). After 16 h, white precipitates were recovered via filtration and dried under vacuum to give compound 7 as a white solid (102 mg, 84% yield). This reaction was similarly successful when it was performed with THF instead of toluene. Single crystals suitable for X-ray diffraction were obtained from a $\text{C}_6\text{H}_5\text{Br}$ /hexanes solution of 7. ^1H NMR (600 MHz, $\text{C}_6\text{D}_5\text{Br}$, 298 K): δ 3.57 (br. s, 6H, N(CH₃)), 1.55 (s, 6H, C(CH₃)). $^{13}\text{C}\{\text{H}\}$ NMR (200 MHz, $\text{C}_6\text{D}_5\text{Br}$, 298 K): δ 178.1, 124.6, 34.6, 8.2.

Synthesis of $(^{\text{Me}}\text{NHC})_3\text{MgBr}_2$ (8a) and $[(^{\text{Me}}\text{NHC})_3\text{MgBr}][\text{Br}]$ (8b). Free $^{\text{Me}}\text{NHC}$ (29 mg, 0.232 mmol) was added to a stirred suspension of 7 (50 mg, 0.116 mmol) in $\text{C}_6\text{H}_5\text{Cl}$ (5 mL). A clear solution was observed after 5 min and was stirred for 1 h at room temperature. After filtration of trace solids, a layer of hexanes was added to the filtrate, precipitating colorless prismlike cocrystallized (1:1) adducts of 8a and 8b at room temperature after 1 day. After removal of the supernatant and drying under vacuum, the product was isolated as an off-white solid (33 mg, 41% yield). An alternative procedure involves the addition of $^{\text{Me}}\text{NHC}$ (70 mg, 0.564 mmol) to a stirred toluene solution of MgBr_2 (30 mg, 0.161 mmol). After 24 h, white solids were recovered via filtration and dried under vacuum (73 mg, 82% yield). Notably, VT-NMR ($\text{C}_6\text{D}_5\text{Br}$, 248–373 K) experiments could not resolve more than one unique product in solution. ^1H NMR (600 MHz, $\text{C}_6\text{D}_5\text{Br}$, 298 K): δ 3.55 (br. s, 6H, N(CH₃)), 1.60 (s, 6H, C(CH₃)). $^{13}\text{C}\{\text{H}\}$ NMR (200 MHz, $\text{C}_6\text{D}_5\text{Br}$, 298 K): δ 124.2, 34.6, 8.3. Due to poor solubility, the carbene carbon resonance was not observed.

Computational Details. The starting geometries of compounds 2, 3, 4, 5, 7, 8a, and 8b were each extracted from the X-ray crystal structures. All density functional theory geometry optimizations and corresponding harmonic vibrational frequency computations were carried out using Gaussian 16 Revision B.01³⁰ at the $\omega\text{B97X-D/BS1}$ level of theory.³¹ The default pruned UltraFine integration grids were used for all energy computations (99 radial shells with 590 points per shell (99590) and pruned SG1 grids using 50 radial shells with 194 points per shell (50194) for Hessians. The default SCF convergence criteria (10^{-8}) was used. The basis set (designated as BS1) utilized cc-pVQZ for Mg, C, O, N, and H and cc-pVQZ-PP for Br.³² For each compound, the Wiberg bond indices (WBI) formulated within the natural atomic orbital (NAO) basis and natural charges were calculated using NBO 3.1, as implemented in Gaussian 09 Revision D.01.³³

ASSOCIATED CONTENT

Supporting Information

The Supporting Information is available free of charge at <https://pubs.acs.org/doi/10.1021/acs.organomet.0c00462>.

Crystal structures of 3[BAr^F₄] and 4[BAr^F₄], NMR spectra, crystallographic refinement details, and computational data (PDF)

Cartesian coordinates for the calculated structures (XYZ)

Accession Codes

CCDC 1998358–1998364 and 2018107 contain the supplementary crystallographic data for this paper. These data can be obtained free of charge via www.ccdc.cam.ac.uk/data_request/cif, or by emailing data_request@ccdc.cam.ac.uk, or by contacting The Cambridge Crystallographic Data Centre, 12 Union Road, Cambridge CB2 1EZ, UK; fax: +44 1223 336033.

AUTHOR INFORMATION

Corresponding Authors

Charles Edwin Webster – Department of Chemistry, Mississippi State University, Mississippi State, Mississippi 39762, United States; orcid.org/0000-0002-6917-2957; Email: cwebster@chemistry.mssstate.edu

Robert J. Gilliard, Jr. – Department of Chemistry, University of Virginia, Charlottesville, Virginia 22904, United States;

✉ orcid.org/0000-0002-8830-1064; Email: rjg8s@virginia.edu

Authors

Akachukwu D. Obi — Department of Chemistry, University of Virginia, Charlottesville, Virginia 22904, United States;

✉ orcid.org/0000-0001-7118-7931

Jacob E. Walley — Department of Chemistry, University of Virginia, Charlottesville, Virginia 22904, United States;

✉ orcid.org/0000-0003-1495-6823

Nathan C. Frey — Department of Chemistry, Mississippi State University, Mississippi State, Mississippi 39762, United States;

✉ orcid.org/0000-0001-7406-1736

Yuen Onn Wong — Department of Chemistry, University of Virginia, Charlottesville, Virginia 22904, United States

Diane A. Dickie — Department of Chemistry, University of Virginia, Charlottesville, Virginia 22904, United States;

✉ orcid.org/0000-0003-0939-3309

Complete contact information is available at:

<https://pubs.acs.org/10.1021/acs.organomet.0c00462>

Author Contributions

The manuscript was written through contributions of all authors. All authors have given approval to the final version of the manuscript.

Notes

The authors declare no competing financial interest.

ACKNOWLEDGMENTS

The authors acknowledge the University of Virginia, the Mississippi State University Office of Research and Economic Development, and the National Science Foundation (OIA-1539035, CHE 1800201, and CHE-1659830) for support of this work. We also thank the MSU High Performance Computing Collaboratory (HPC²) and the Mississippi Center for Supercomputing Research (MCSR) for the use of computational resources.

REFERENCES

(1) (a) Hill, M. S.; Liptrot, D. J.; Weetman, C. Alkaline earths as main group reagents in molecular catalysis. *Chem. Soc. Rev.* **2016**, *45*, 972–988. (b) Harder, S. *Alkaline-earth metal compounds: oddities and applications*; Springer Berlin Heidelberg: Berlin, 2013; Vol. 45. (c) Harder, S. *Early Main Group Metal Catalysis: Concepts and Reactions*; Wiley-VCH: Weinheim, Germany, 2020.

(2) (a) Stasch, A.; Jones, C. Stable dimeric magnesium(I) compounds: from chemical landmarks to versatile reagents. *Dalton Trans.* **2011**, *40*, 5659–5672. (b) Jones, C. Dimeric magnesium(I) β -diketiminates: a new class of quasi-universal reducing agent. *Nat. Rev. Chem.* **2017**, *1*, 0059. (c) Penafiel, J.; Maron, L.; Harder, S. Early main group metal catalysis: how important is the metal? *Angew. Chem., Int. Ed.* **2015**, *54*, 201–206. (d) Harder, S., Introduction to Early Main Group Organometallic Chemistry and Catalysis. In *Early Main Group Metal Catalysis*, Harder, S., Ed.; Wiley: 2020; pp 1–29. (e) Rauch, M.; Parkin, G. Zinc and Magnesium Catalysts for the Hydrosilylation of Carbon Dioxide. *J. Am. Chem. Soc.* **2017**, *139*, 18162–18165.

(3) (a) Wilson, A. S. S.; Dinoi, C.; Hill, M. S.; Mahon, M. F.; Maron, L. Heterolysis of Dihydrogen by Nucleophilic Calcium Alkyls. *Angew. Chem., Int. Ed.* **2018**, *57*, 15500–15504. (b) Anker, M. D.; Arrowsmith, M.; Bellham, P.; Hill, M. S.; Kociok-Köhn, G.; Liptrot, D. J.; Mahon, M. F.; Weetman, C. Selective reduction of CO₂ to a methanol equivalent by B(C₆FS)₃-activated alkaline earth catalysis. *Chem. Sci.* **2014**, *5*, 2826–2830. (c) Brand, S.; Elsen, H.; Langer, J.; Grams, S.; Harder, S. Calcium-Catalyzed Arene C–H Bond Activation by Low-Valent AlI. *Angew. Chem., Int. Ed.* **2019**, *58*, 15496–15503. (d) Wilson, A. S. S.; Hill, M. S.; Mahon, M. F.; Dinoi, C.; Maron, L. Organocalcium-mediated nucleophilic alkylation of benzene. *Science* **2017**, *358*, 1168–1171. (e) Garcia, L.; Dinoi, C.; Mahon, M. F.; Maron, L.; Hill, M. S. Magnesium hydride alkene insertion and catalytic hydrosilylation. *Chem. Sci.* **2019**, *10*, 8108–8118.

(4) (a) Pahl, J.; Brand, S.; Elsen, H.; Harder, S. Highly Lewis acidic cationic alkaline earth metal complexes. *Chem. Commun.* **2018**, *54*, 8685–8688. (b) Garcia, L.; Anker, M. D.; Mahon, M. F.; Maron, L.; Hill, M. S. Coordination of arenes and phosphines by charge separated alkaline earth cations. *Dalton Trans.* **2018**, *47*, 12684–12693. (c) Pahl, J.; Elsen, H.; Friedrich, A.; Harder, S. Unsupported metal silyl ether coordination. *Chem. Commun.* **2018**, *54*, 7846–7849. (d) Schwamm, R. J.; Coles, M. P.; Hill, M. S.; Mahon, M. F.; McMullin, C. L.; Rajabi, N. A.; Wilson, A. S. S. A Stable Calcium Alumanyl. *Angew. Chem., Int. Ed.* **2020**, *59*, 3928–3932. (e) Pahl, J.; Friedrich, A.; Elsen, H.; Harder, S. Cationic Magnesium π -Arene Complexes. *Organometallics* **2018**, *37*, 2901–2909. (f) Pahl, J.; Stennett, T. E.; Volland, M.; Guldi, D. M.; Harder, S. Complexation and Versatile Reactivity of a Highly Lewis Acidic Cationic Mg Complex with Alkynes and Phosphines. *Chem. - Eur. J.* **2019**, *25*, 2025–2034. (g) Friedrich, A.; Pahl, J.; Elsen, H.; Harder, S. Bulky cationic beta-diketiminate magnesium complexes. *Dalton Trans.* **2019**, *48*, 5560–5568.

(5) Brand, S.; Elsen, H.; Langer, J.; Donaubauer, W. A.; Hampel, F.; Harder, S. Facile Benzene Reduction by a Ca²⁺/AlI Lewis Acid/Base Combination. *Angew. Chem., Int. Ed.* **2018**, *57*, 14169–14173.

(6) Garcia, L.; Mahon, M. F.; Hill, M. S. Multimetallic Alkaline-Earth Hydride Cations. *Organometallics* **2019**, *38*, 3778–3785.

(7) (a) Lemmerz, L. E.; Mukherjee, D.; Spaniol, T. P.; Wong, A.; Ménard, G.; Maron, L.; Okuda, J. Cationic magnesium hydride [MgH]_n stabilized by an NNNN-type macrocycle. *Chem. Commun.* **2019**, *55*, 3199–3202. (b) Leich, V.; Spaniol, T. P.; Maron, L.; Okuda, J. Molecular Calcium Hydride: Dicalcium Trihydride Cation Stabilized by a Neutral NNNN-Type Macroyclic Ligand. *Angew. Chem., Int. Ed.* **2016**, *55*, 4794–4797. (c) Bruyere, J.-C.; Gourlaouen, C.; Karmazin, L.; Bailly, C.; Boudon, C.; Ruhlmann, L.; de Frémont, P.; Dagorne, S. Synthesis and Characterization of Neutral and Cationic Magnesium Complexes Supported by NHC Ligands. *Organometallics* **2019**, *38*, 2748–2757. (d) Herrmann, W. A.; Runte, O.; Artus, G. Synthesis and structure of an ionic beryllium-“carbene” complex. *J. Organomet. Chem.* **1995**, *501*, C1–C4.

(8) (a) Arduengo, A. J.; Harlow, R. L.; Kline, M. A stable crystalline carbene. *J. Am. Chem. Soc.* **1991**, *113*, 361–363. (b) Arduengo, A. J.; Krafczyk, R.; Schmutzler, R.; Craig, H. A.; Goerlich, J. R.; Marshall, W. J.; Unverzagt, M. Imidazolylidene, imidazolinylidene and imidazolidinylidene. *Tetrahedron* **1999**, *55*, 14523–14534. (c) Lavallo, V.; Canac, Y.; Prasang, C.; Donnadieu, B.; Bertrand, G. Stable cyclic (alkyl)(amino)-carbenes as rigid or flexible, bulky, electron-rich ligands for transition-metal catalysts: a quaternary carbon atom makes the difference. *Angew. Chem., Int. Ed.* **2005**, *44*, 5705–5709. (d) Soleilhavoup, M.; Bertrand, G. Cyclic (alkyl)(amino)carbenes (CAACs): stable carbenes on the rise. *Acc. Chem. Res.* **2015**, *48*, 256–266. (e) Melaimi, M.; Jazairi, R.; Soleilhavoup, M.; Bertrand, G. Cyclic (Alkyl)(amino)carbenes (CAACs): Recent Developments. *Angew. Chem., Int. Ed.* **2017**, *56*, 10046–10068. (f) Munz, D. Pushing Electrons—Which Carbene Ligand for Which Application? *Organometallics* **2018**, *37*, 275–289.

(9) Selected reviews: (a) Bourissou, D.; Guerret, O.; Gabbaï, F. P.; Bertrand, G. Stable Carbenes. *Chem. Rev.* **2000**, *100*, 39–92. (b) Diez-Gonzalez, S.; Marion, N.; Nolan, S. P. N-heterocyclic carbenes in late transition metal catalysis. *Chem. Rev.* **2009**, *109*, 3612–3676. (c) Hopkinson, M. N.; Richter, C.; Schedler, M.; Glorius, F. An overview of N-heterocyclic carbenes. *Nature* **2014**, *510*, 485–496. (d) Nesterov, V.; Reiter, D.; Bag, P.; Frisch, P.; Holzner, R.; Porzelt, A.; Inoue, S. NHCs in Main Group Chemistry. *Chem. Rev.* **2018**, *118*, 9678–9842. (e) Bellemin-Laponnaz, S.; Dagorne, S. Group 1 and 2 and Early Transition Metal Complexes Bearing N-Heterocyclic Carbene Ligands: Coordination Chemistry, Reactivity, and Applications. *Chem. Rev.* **2014**, *114*, 8747–8774. (f) Zhao, Q.; Meng, G.; Nolan, S. P.; Szostak, M. N-Heterocyclic Carbene Complexes in C–H Activation Reactions. *Chem. Rev.* **2020**, *120*, 1981–2048. (g) Groom, C. R.

Bruno, I. J.; Lightfoot, M. P.; Ward, S. C. The Cambridge Structural Database. *Acta Crystallogr., Sect. B: Struct. Sci., Cryst. Eng. Mater.* **2016**, *72*, 171–179.

(10) Seyerth, D. The Grignard Reagents. *Organometallics* **2009**, *28*, 1598–1605.

(11) See ref 9d for a recent review. Selected examples: (a) Wang, G.; Walley, J. E.; Dickie, D. A.; Pan, S.; Frenking, G.; Gilliard, R. J.; Stable, A. Crystalline Beryllium Radical Cation. *J. Am. Chem. Soc.* **2020**, *142*, 4560–4564. (b) Arrowsmith, M.; Hill, M. S.; Kociok-Kohn, G.; MacDougall, D. J.; Mahon, M. F. Beryllium-induced C–N bond activation and ring opening of an N-heterocyclic carbene. *Angew. Chem., Int. Ed.* **2012**, *51*, 2098–2100. (c) Arrowsmith, M.; Braunschweig, H.; Celik, M. A.; Dellermann, T.; Dewhurst, R. D.; Ewing, W. C.; Hammond, K.; Kramer, T.; Krummenacher, I.; Mies, J.; Radacki, K.; Schuster, J. K. Neutral zero-valent s-block complexes with strong multiple bonding. *Nat. Chem.* **2016**, *8*, 890–894. (d) Wang, G.; Freeman, L. A.; Dickie, D. A.; Mokrai, R.; Benkő, Z.; Gilliard, R. J. Isolation of Cyclic(Alkyl)(Amino) Carbene–Bismuthinidene Mediated by a Beryllium(0) Complex. *Chem. - Eur. J.* **2019**, *25*, 4335–4339. (e) Martínez-Martínez, A. J.; Fuentes, M. A.; Hernán-Gómez, A.; Hevia, E.; Kennedy, A. R.; Mulvey, R. E.; O’Hara, C. T. Alkali-Metal-Mediated Magnesiations of an N-Heterocyclic Carbene: Normal, Abnormal, and “Paranormal” Reactivity in a Single Tropic Molecule. *Angew. Chem., Int. Ed.* **2015**, *54*, 14075–14079. (f) Yuvaraj, K.; Douair, I.; Paparo, A.; Maron, L.; Jones, C. Reductive Trimerization of CO to the Deltate Dianion Using Activated Magnesium(I) Compounds. *J. Am. Chem. Soc.* **2019**, *141*, 8764–8768. (g) Arrowsmith, M.; Hill, M. S.; MacDougall, D. J.; Mahon, M. F. A hydride-rich magnesium cluster. *Angew. Chem., Int. Ed.* **2009**, *48*, 4013–4016. (h) Jones, C.; Yuvaraj, K.; Douair, I.; Maron, L. Activation of Ethylene by N-Heterocyclic Carbene Coordinated Magnesium(I) Compounds. *Chem. - Eur. J.* **2020**, DOI: 10.1002/chem.202002380. (i) Paparo, A.; Best, S. P.; Yuvaraj, K.; Jones, C. Neutral, Anionic, and Paramagnetic 1,3,2-Diazaberyllacycles Derived from Reduced 1,4-Diazabutadienes. *Organometallics* **2020**, DOI: 10.1021/acs.organomet.0c00017. (j) Arrowsmith, M.; Hill, M. S.; Kociok-Kohn, G. Activation of N-Heterocyclic Carbene by {BeH₂} and {Be(H)(Me)} Fragments. *Organometallics* **2015**, *34*, 653–662.

(12) (a) Wong, Y. O.; Freeman, L. A.; Agakidou, A. D.; Dickie, D. A.; Webster, C. E.; Gilliard, R. J. Two Carbenes versus One in Magnesium Chemistry: Synthesis of Terminal Dihalide, Dialkyl, and Grignard Reagents. *Organometallics* **2019**, *38*, 688–696. (b) Freeman, L. A.; Walley, J. E.; Obi, A. D.; Wang, G.; Dickie, D. A.; Molino, A.; Wilson, D. J. D.; Gilliard, R. J. Stepwise Reduction at Magnesium and Beryllium: Cooperative Effects of Carbenes with Redox Non-Innocent α -Diimines. *Inorg. Chem.* **2019**, *58*, 10554–10568. (c) Walley, J. E.; Wong, Y.-O.; Freeman, L. A.; Dickie, D. A.; Gilliard, R. J. N-Heterocyclic Carbene-Supported Aryl and Alk-oxides of Beryllium and Magnesium. *Catalysts* **2019**, *9*, 934–945. (d) Freeman, L. A.; Walley, J. E.; Dickie, D. A.; Gilliard, R. J. Low-nuclearity magnesium hydride complexes stabilized by N-heterocyclic carbenes. *Dalton Trans.* **2019**, *48*, 17174–17178. (e) Walley, J. E.; Obi, A. D.; Breiner, G.; Wang, G.; Dickie, D. A.; Molino, A.; Dutton, J. L.; Wilson, D. J. D.; Gilliard, R. J. Cyclic(alkyl)(amino) Carbene-Promoted Ring Expansion of a Carbodicarbene Beryllacycle. *Inorg. Chem.* **2019**, *58*, 11118–11126.

(13) Kennedy, A. R.; Mulvey, R. E.; Robertson, S. D. N-Heterocyclic carbene stabilized adducts of alkyl magnesium amide, bisalkyl magnesium and Grignard reagents: trapping oligomeric organo s-block fragments with NHCs. *Dalton Trans.* **2010**, *39*, 9091–9099.

(14) In this article, bis- and tris(carbene) stabilizations refer to the coordination of two or three untethered carbene units to a single magnesium atom. This notation is also used in the literature for neutral or anionic chelates housing tethered NHC units. Indeed, there exists only one example of tethered tris(NHC) coordination to magnesium. See: Nieto, I.; Cervantes-Lee, F.; Smith, J. M. A new synthetic route to bulky “second generation” tris(imidazol-2-ylidene)borate ligands: synthesis of a four coordinate iron(ii) complex. *Chem. Commun.* **2005**, 3811–3813.

(15) (a) Bailey, P. J.; Coxall, R. A.; Dick, C. M.; Fabre, S.; Parsons, S.; Yellowlees, L. J. Structural and EPR characterisation of single electron and alkyl transfer products from reaction of dimethyl magnesium with bulky α -diimine ligands. *Chem. Commun.* **2005**, 4563–4565. (b) Gibson, V. C.; Segal, J. A.; White, A. J. P.; Williams, D. J. Novel Mono-alkyl Magnesium Complexes Stabilized by a Bulky β -Diketiminate Ligand: Structural Characterization of a Coordinatively Unsaturated Trigonal System. *J. Am. Chem. Soc.* **2000**, *122*, 7120–7121. (c) Bailey, P. J.; Dick, C. M. E.; Fabre, S.; Parsons, S. Synthesis and characterisation of magnesium methyl complexes with monoanionic chelating nitrogen donor ligands and their reaction with dioxygen. *J. Chem. Soc., Dalton Trans.* **2000**, 1655–1661. (d) Stuhl, C.; Anwander, R. Dimethylmagnesium revisited. *Dalton Trans.* **2018**, *47*, 12546–12552. (e) Michel, O.; Meermann, C.; Törnroos, K. W.; Anwander, R. Alkaline-Earth Metal Alkylaluminate Chemistry Revisited. *Organometallics* **2009**, *28*, 4783–4790.

(16) Viebrock, H.; Behrens, U.; Weiss, E. A Novel Organomagnesium Compound Consisting of Two Triple-Decker Cations [LMg(μ -Me₃)MgL]⁺ and an Octamethyltrimagnesate Anion: [{Me₂Mg(μ -Me)₂}₂Mg]²⁻. *Angew. Chem., Int. Ed. Engl.* **1994**, *33*, 1257–1259.

(17) (a) Peltzer, R. M.; Eisenstein, O.; Nova, A.; Cascella, M. How Solvent Dynamics Controls the Schlenk Equilibrium of Grignard Reagents: A Computational Study of CH₃MgCl in Tetrahydrofuran. *J. Phys. Chem. B* **2017**, *121*, 4226–4237. (b) Peltzer, R. M.; Gauss, J.; Eisenstein, O.; Cascella, M. The Grignard Reaction – Unraveling a Chemical Puzzle. *J. Am. Chem. Soc.* **2020**, *142*, 2984–2994.

(18) Obi, A. D.; Dickie, D. A.; Gilliard, R. J. CCDC 2009525: Experimental Crystal Structure Determination. *CSD Communication* **2020**.

(19) Kuhn, N.; Kratz, T. Synthesis of Imidazol-2-ylidenes by Reduction of Imidazole-2(3H)-thiones. *Synthesis* **1993**, *1993*, 561–562.

(20) Pyykkö, P.; Atsumi, M. Molecular Single-Bond Covalent Radii for Elements 1–118. *Chem. - Eur. J.* **2009**, *15*, 186–197.

(21) Mantina, M.; Chamberlin, A. C.; Valero, R.; Cramer, C. J.; Truhlar, D. G. Consistent van der Waals Radii for the Whole Main Group. *J. Phys. Chem. A* **2009**, *113*, 5806–5812.

(22) (a) Couchman, S. A.; Holzmann, N.; Frenking, G.; Wilson, D. J.; Dutton, J. L. Beryllium chemistry the safe way: a theoretical evaluation of low oxidation state beryllium compounds. *Dalton Trans.* **2013**, *42*, 11375–11384. (b) De, S.; Parameswaran, P. Neutral tricoordinated beryllium(0) compounds – isostructural to BH₃ but isoelectronic to NH₃. *Dalton Trans.* **2013**, *42*, 4650–4656.

(23) (a) Rit, A.; Zanardi, A.; Spaniol, T. P.; Maron, L.; Okuda, J. A Cationic Zinc Hydride Cluster Stabilized by an N-Heterocyclic Carbene: Synthesis, Reactivity, and Hydrosilylation Catalysis. *Angew. Chem., Int. Ed.* **2014**, *53*, 13273–13277. (b) Schnitzler, S.; Spaniol, T. P.; Maron, L.; Okuda, J. Formation and Reactivity of a Molecular Magnesium Hydride with a Terminal Mg–H Bond. *Chem. - Eur. J.* **2015**, *21*, 11330–11334.

(24) Sheldrick, G. M. SHELXT – Integrated space-group and crystal-structure determination. *Acta Crystallogr., Sect. A: Found. Adv.* **2015**, *71*, 3–8.

(25) Saint, SADABS, APEX3; Bruker AXS Inc.: Madison, WI, USA, 2012.

(26) Dolomanov, O. V.; Bourhis, L. J.; Gildea, R. J.; Howard, J. A. K.; Puschmann, H. OLEX2: a complete structure solution, refinement and analysis program. *J. Appl. Crystallogr.* **2009**, *42*, 339–341.

(27) Yakelis, N. A.; Bergman, R. G. Safe Preparation and Purification of Sodium Tetrakis[(3,5-trifluoromethyl)phenyl]borate (NaBArF₂₄): Reliable and Sensitive Analysis of Water in Solutions of Fluorinated Tetraarylborates. *Organometallics* **2005**, *24*, 3579–3581.

(28) Ansell, M. B.; Roberts, D. E.; Cloke, F. G. N.; Navarro, O.; Spencer, J. Synthesis of an [(NHC)Pd(SiMe₃)₂] Complex and Catalytic cis-Bis(silyl)ations of Alkynes with Unactivated Disilanes. *Angew. Chem., Int. Ed.* **2015**, *54*, 5578–5582.

(29) (a) Bailey, P. J.; Dick, C. M.; Fabre, S.; Parsons, S.; Yellowlees, L. J. Complexation of dimethylmagnesium with alpha-diimines; structural and EPR characterisation of single electron and alkyl transfer products.

Dalton Trans. **2006**, 1602–1610. (b) Vargas, W.; Englisch, U.; Ruhlandt-Senge, K. A Novel Group of Alkaline Earth Metal Amides: Syntheses and Characterization of $M[N(2,6-iPr_2C_6H_3)(SiMe_3)]_2 \cdot (THF)_2$ ($M = Mg, Ca, Sr, Ba$) and the Linear, Two-Coordinate $Mg[N(2,6-iPr_2C_6H_3)(SiMe_3)]_2$. *Inorg. Chem.* **2002**, *41*, 5602–5608. (c) Hays, M. L.; Hanusa, T. P.; Nile, T. A. Synthesis and X-ray crystal structures of alkaline-earth metallocenes with pendant substituents. *J. Organomet. Chem.* **1996**, *514*, 73–79.

(30) Frisch, M. J.; Trucks, G. W.; Schlegel, H. B.; Scuseria, G. E.; Robb, M. A.; Cheeseman, J. R.; Scalmani, G.; Barone, V.; Petersson, G. A.; Nakatsuji, H.; Li, X.; Caricato, M.; Marenich, A. V.; Bloino, J.; Janesko, B. G.; Gomperts, R.; Mennucci, B.; Hratchian, H. P.; Ortiz, J. V.; Izmaylov, A. F.; Sonnenberg, J. L.; Williams, Ding, F.; Lipparini, F.; Egidi, F.; Goings, J.; Peng, B.; Petrone, A.; Henderson, T.; Ranasinghe, D.; Zakrzewski, V. G.; Gao, J.; Rega, N.; Zheng, G.; Liang, W.; Hada, M.; Ehara, M.; Toyota, K.; Fukuda, R.; Hasegawa, J.; Ishida, M.; Nakajima, T.; Honda, Y.; Kitao, O.; Nakai, H.; Vreven, T.; Throssell, K.; Montgomery, J. A., Jr.; Peralta, J. E.; Ogliaro, F.; Bearpark, M. J.; Heyd, J. J.; Brothers, E. N.; Kudin, K. N.; Staroverov, V. N.; Keith, T. A.; Kobayashi, R.; Normand, J.; Raghavachari, K.; Rendell, A. P.; Burant, J. C.; Iyengar, S. S.; Tomasi, J.; Cossi, M.; Millam, J. M.; Klene, M.; Adamo, C.; Cammi, R.; Ochterski, J. W.; Martin, R. L.; Morokuma, K.; Farkas, O.; Foresman, J. B.; Fox, D. J. *Gaussian 16, Rev. B.01*; Gaussian Inc.: Wallingford, CT, 2016.

(31) Chai, J.-D.; Head-Gordon, M. Long-range corrected hybrid density functionals with damped atom–atom dispersion corrections. *Phys. Chem. Chem. Phys.* **2008**, *10*, 6615–6620.

(32) (a) Kendall, R. A.; Dunning, T. H.; Harrison, R. J. Electron affinities of the first-row atoms revisited. Systematic basis sets and wave functions. *J. Chem. Phys.* **1992**, *96*, 6796–6806. (b) Dunning, T. H., Jr Gaussian basis sets for use in correlated molecular calculations. I. The atoms boron through neon and hydrogen. *J. Chem. Phys.* **1989**, *90*, 1007–1023. (c) Peterson, K. A.; Shepler, B. C.; Figgen, D.; Stoll, H. On the Spectroscopic and Thermochemical Properties of ClO , BrO , IO , and Their Anions. *J. Phys. Chem. A* **2006**, *110*, 13877–13883. (d) Peterson, K. A. Systematically convergent basis sets with relativistic pseudopotentials. I. Correlation consistent basis sets for the post-d group 13–15 elements. *J. Chem. Phys.* **2003**, *119*, 11099–11112. (e) Peterson, K. A.; Figgen, D.; Goll, E.; Stoll, H.; Dolg, M. Systematically convergent basis sets with relativistic pseudopotentials. II. Small-core pseudopotentials and correlation consistent basis sets for the post-d group 16–18 elements. *J. Chem. Phys.* **2003**, *119*, 11113–11123.

(33) Frisch, M. J.; Trucks, G. W.; Schlegel, H. B.; Scuseria, G. E.; Robb, M. A.; Cheeseman, J. R.; Scalmani, G.; Barone, V.; Petersson, G. A.; Nakatsuji, H.; Li, X.; Caricato, M.; Marenich, A. V.; Bloino, J.; Janesko, B. G.; Gomperts, R.; Mennucci, B.; Hratchian, H. P.; Ortiz, J. V.; Izmaylov, A. F.; Sonnenberg, J. L.; Williams, Ding, F.; Lipparini, F.; Egidi, F.; Goings, J.; Peng, B.; Petrone, A.; Henderson, T.; Ranasinghe, D.; Zakrzewski, V. G.; Gao, J.; Rega, N.; Zheng, G.; Liang, W.; Hada, M.; Ehara, M.; Toyota, K.; Fukuda, R.; Hasegawa, J.; Ishida, M.; Nakajima, T.; Honda, Y.; Kitao, O.; Nakai, H.; Vreven, T.; Throssell, K.; Montgomery, J. A., Jr.; Peralta, J. E.; Ogliaro, F.; Bearpark, M. J.; Heyd, J. J.; Brothers, E. N.; Kudin, K. N.; Staroverov, V. N.; Keith, T. A.; Kobayashi, R.; Normand, J.; Raghavachari, K.; Rendell, A. P.; Burant, J. C.; Iyengar, S. S.; Tomasi, J.; Cossi, M.; Millam, J. M.; Klene, M.; Adamo, C.; Cammi, R.; Ochterski, J. W.; Martin, R. L.; Morokuma, K.; Farkas, O.; Foresman, J. B.; Fox, D. J. *Gaussian 09, Rev. D.01*; Gaussian Inc.: Wallingford, CT, 2016.